THEORETICAL AND EXPERIMENTAL VALIDATION OF HYDROGEN FUELED SPARK IGNITION ENGINE

by

Ganapathy Pandian SAKTHINATHAN [a*]
and Krishnamoorthy JEYACHANDRAN [b]

[a] Department of Manufacturing Engineering, Anna University, Chennai, India
[b] Mechanical Engineering Department, Anna University, Chennai, India

Original scientific paper
UDC: 662.769.2:66.011/.012
DOI: 10.2298/TSCI1004989S

In modern research, simulation has become a powerful tool as it saves time and also economical when compared to experimental study. This paper deals with a comprehensive model of a spark ignition hydrogen fueled engine. Woschni's heat transfer co-relation is used by this model for predicting the heat transfer in the engine. Two zone combustion model has been opted for simulating the combustion process. Two zone models account for the combustion chamber geometry and for the presence of burnt and unburnt gases. The results are compared with the experimental data and it is found that there was a good convergence of results. The engine efficiency and power has been slightly over predicted because dissociation has not been included in the model.

Key words: *simulation, hydrogen, Woschni's combustion model, heat release, rate,* NO_x *emission*

Introduction

Considering the energy crisis and pollution problems, investigations have been concentrating on reducing the fuel consumption and lowering the concentration of toxic components in combustion products by opting for alternative fuels. Hydrogen is considered as an ideal alternative fuel. Many researchers have studied engine performance and emission by using hydrogen as a fuel. Hydrogen has been recognized as an alternate fuel as it has highly desirable properties. It is the only fuel that can be produced from the plentiful renewal source water. Its combustion in oxygen produces only water but in air it also produces oxides of nitrogen. Hydrogen mixes very easily with air to form mixture as lean as 4% and as rich as 75% in volume basis having wide flammability limits [1].

Hydrogen can be easily ignited and the flame speed is about nine times that of gasoline. Computer simulation of internal combustion engines are desirable because of the aid they provide in design, in predicting the trends, in serving as diagnostics tools, in giving more data than are normally obtainable from the experiment, and in helping to understand the complex processes that occur inside the engine. It also reduces the time involved for the experimental in-

* Corresponding author; e-mail: gsakthinathan@annauniv.edu

vestigation and the cost involved. Simulation of IC engine processes involves, developing a combustion model using the combination of assumptions and equations for predicting the engine performance during the open period which involves suction and exhaust strokes and the closed period which comprises compression, combustion, and expansion stroke. The objective of the present study is to develop a combustion model for a spark ignition engine running with hydrogen as a fuel and predicting its behavior.

Thermodynamic model

Thermodynamic analysis of the hydrogen fueled engine is considered for closed period during which both inlet and exhaust valves remain closed. The important events such as compression, combustion, and expansion take place during this period. The engine is reduced to a thermodynamic system, which consist of a homogenous mixture of air, hydrogen, and residual gas from the previous cycle. The boundaries of the system are the cylinder walls, cylinder head, and top of the piston head. Work is added to or taken from the system through the motion of the piston and heat is transferred to or from the system through the boundary surfaces. Thermodynamic models can be classified into two subgroups; single zone model and multizone model. In single zone models, the cylinder charge (*i. e.*, the mixture in the cylinder) is assumed to be uniform in both composition and temperature and the first law of thermodynamics is used to calculate the mixture energy. But in this study, two zone models has been selected and used for analysis. In two zone model, the cylinder mixture is divided into burnt and unburnt zones, which are separate from each other by a surface of discontinuity. The composition and temperature of the burnt and unburnt gases are different and the pressure is uniform throughout the combustion chamber.

Assumptions

In this model, the folowing assumptions have been used.

- The charge in the cylinder at any instant consists of fuel-air mixture and residual gases. Ideal gas equation is assumed to be valid for the mixture of gases.
- There are no deposits on the walls of the combustion chamber.
- Heat transfer takes place through three surfaces (a) the cylinder head (b) the piston, and (c) the exposed sleeve area.
- Cylinder volume at any instant consists of burnt and unburnt zones separated by a thin infinitesimal flame front.
- The pressure is constant for both the zones.
- The burnt and unburnt gases are assumed to be ideal and non-reacting. The heat transfer from the burnt to unburnt gases is assumed to be negligible. The rate of heat transfer from gas to the wall depends on instantaneous heat transfer coefficient, concerned surface area, and difference in temperature between the gas and wall.
- Flame propagates in a spherical pattern.
- There is assumed to be no dissociation in the unburnt gases prior to combustion.

Compression process

During the compression process the combustion chamber contains homogeneous air fuel-mixture and residual gases only. In the first iteration, residual gas fraction within the cylinder was assumed to be zero, and residual gas fraction obtained at the end of first iteration was used in subsequent iterations.

For the closed system, the basic energy equation combined with characteristic gas equation can be written as:

$$\dot{U} \quad \frac{m\mathrm{R}T}{V}\dot{V} \quad \Sigma Q_{\mathrm{i}} \tag{1}$$

The first term on the right hand side consists of the volume and its derivative, which could be obtained from the volume at any instant from the geometrical relation. The second term on the right hand side of eq. (1) deals with the estimation of the heat transfer rate.

The term on the left hand side indicates the rate of change internal energy to time. The internal energy at any instant is assumed to be a function of temperature only. It is given by:

$$\dot{U} \quad mC_{\mathrm{v}}\frac{\mathrm{d}T}{\mathrm{d}\theta} \tag{2}$$

Now the eq. (1) becomes

$$\frac{\mathrm{d}T}{\mathrm{d}\theta} \quad [\ P\dot{V} \quad h_{\mathrm{i}}A_{\mathrm{i}}(T_{\mathrm{w}} \quad T)]\frac{1}{mC_{\mathrm{v}}} \tag{3}$$

Volume calculations

The total volume of the gases inside the cylinder at a particular crank angle θ is given by the expression:

$$V(\theta) \quad V_{\mathrm{disp}}\ \frac{r}{r \quad 1} \quad \frac{1 \quad \cos\theta}{2} \quad \frac{L}{S} \quad \frac{1}{2}\sqrt{\frac{2L}{S}^{2} \quad \sin^{2}\theta} \tag{4}$$

and its derivative is given by:

$$\dot{V}(\theta) \quad \frac{\mathrm{d}V}{\mathrm{d}\theta} \quad \frac{V_{\mathrm{disp}}}{2} \quad \frac{1}{2}\frac{\sin 2\theta}{\sqrt{\frac{2L}{S}^{2} \quad \sin^{2}\theta}} \quad \sin\theta \tag{5}$$

Heat transfer

The method of computation of heat transfer coefficient due to convection is the key factor which controls the order of magnitude of the rate of heat transfer. Heat transfer by convection is given by:

$$Q_{\mathrm{i}} = h_{\mathrm{i}}A_{\mathrm{i}}(T_{\mathrm{w}} - T) \tag{6}$$

Area of heat transfer surfaces

During the closed period, the heat transfer area of exposed surfaces such as head, piston is constant except the sleeve surfaces which should be vary with respect to crank angle. The instantaneous sleeve surface area is calculated as follows.

From the engine kinematics, the distance between the cylinder head and the piston could be written as:

$$L(\theta) \quad L \quad \frac{S}{2} \quad L\sqrt{1 \quad \frac{S^2 \sin^2\theta}{4L^2}} \quad \frac{S}{2}\cos\theta \tag{7}$$

The area of sleeve at any instant:

$$A_S = \pi B L(\theta) \tag{8}$$

So the total area for the heat transfer is reduced to

$$A_{Total} = \text{Sleeve} + \text{Piston} + \text{Cylinder area} = A_S + A_P + A_H \tag{9}$$

Heat transfer coefficient

The instantaneous heat transfer coefficient h_i is estimated by Woschni's heat transfer co-relation [2] and is given by

$$\begin{aligned} h_i \quad & 0.013B^{\;0.2}P^{0.8}T_g^{\;0.53}w^{0.8} \\ w \quad & 2.28C_m \quad 0.00324(P \quad P_m)\frac{V_h T_r}{P_r V_r} \end{aligned} \tag{10}$$

The heat transfer coefficient obtained from this relation was assumed to be same for all the surfaces of the cylinder.

Cylinder wall temperature

The wall temperature is assumed to be constant throughout the calculation and is given by the equation [3]

$$T_w \quad 300 \quad 25(\sqrt{r} \quad \sqrt[4]{N}) \tag{11}$$

Determination of C_P and C_V of the charge

C_P, C_V, and the ratio of the specific heats γ, based on the charge composition and temperature are calculated by using the polynomial equations as a function of temperature:

$$\frac{C_P}{R} \quad a_1 \quad a_2T \quad a_3T^2 \quad a_4T^3 \quad a_5T^4 \tag{12}$$

The air fuel ratio for a given operating condition fixes the concentration of species like CO_2, H_2O, H_2, N_2, and O_2. C_p and C_v values for each constituent gas is calculated by using the polynomial equation depending on the range of temperature and the mean value of the products of combustion is calculated by using the equation:

$$C_{Pmix} = \Sigma y_i C_{Pi} \tag{13}$$

where y_i is the number of moles of any of the gases such as CO_2, H_2O, H_2, N_2, and O_2. Finally,

$$C_{Vmix} = C_{Pmix} - \mathrm{R} \tag{14}$$

This procedure also helps in determination of γ, as a function of T throughout the cycle and can be used wherever appropriate. The compression process is assumed to spread over from inlet valve closing to the point of injection. For each crank angle depending on air fuel ratio the mass of the reactants are found out, the heat transfer rate, pressure, and temperature are computed. Knowing the temperature, the specific heat is obtained. This process was carried out till the fuel injection has started. The combustion process is assumed to progress from this instant. From the start of compression during the compression process, the solution of eq. (3) gives the temperature difference ΔT at crank angle θ. This helps in the determination of temperature T at $\theta + 1$ by algebraic addition of T and ΔT. Pressure at $P_{\theta+1}$ is determined. This process is continued from the start of compression to the start of combustion during compression process.

Combustion process

Two zone combustion model

To simulate the combustion process two zone combustion model has been selected as stated earlier. Two zone models account for the combustion chamber geometry and for the presence of burnt and unburnt gases (fig. 1). Although the assumption of uniform temperature in the unburnt gases is reasonable, significant temperature gradients may exist in the burnt gases due to the differences between first burning and then compressing the burnt gas, as compared to first compressing and then burning the fresh mixture.

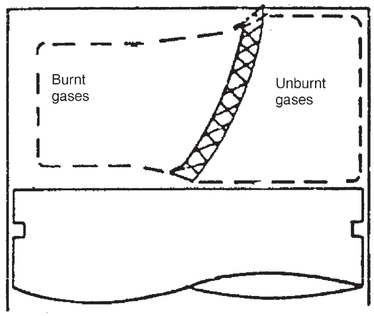

Figure 1. Two zone thermodynamic model

The governing equation for the burnt and unburnt-gas zones can be written as:

$$m = m_u + m_b \tag{15}$$

$$\frac{dm}{d\theta} \quad \frac{dm_u}{d\theta} \quad \frac{dm_b}{d\theta} \tag{16}$$

$$V = V_u + V_b \tag{17}$$

where the subscripts u and b denote the unburnt and burnt gases, respectively.

The folowing system of equations:

$$m_u C_{v_u} \frac{dT_u}{d\theta} \qquad p\frac{dV_u}{d\theta} \quad \frac{dQ_u}{d\theta} \quad h_u \frac{dm_u}{d\theta} \tag{18}$$

$$m_b C_{v_b} \frac{dT_b}{d\theta} \qquad p\frac{dV_b}{d\theta} \quad \frac{dQ_b}{d\theta} \quad h_b \frac{dm_b}{d\theta} \tag{19}$$

$$Q_u = hA_u(T_w - T_u) \tag{20}$$

$$Q_b = hA_b(T_w - T_b) \tag{21}$$

is not closed (*i. e.*, there are more unknowns than equations). Closure can be achieved by specifying the mass burning rate $dm_b/d\theta$ and the geometry of the flame front.

Expressions for flame velocity

Different approaches to specifying a turbulent flame speed in reciprocating engine combustion have been used by various workers. In general, for turbulent combustion in a closed vessel the effects of temperature and stoichiometry are accounted for through a laminar flame speed, and the turbulent flame speed is determined by multiplying this laminar speed by a factor which depends upon the intensity of turbulence [4]. For engine combustion the flame speed is observed to increase with engine speed, so the ratio or turbulent to laminar flame speed must involve the engine speed. The semi-empirical turbulent speed equation is [5]:

$$S_\mathrm{T} = \mathrm{ARe}^\mathrm{B} S_\mathrm{L} \tag{22}$$

In this expression A and B are empirically determined constants [4]. Re is the Reynolds number based on the piston diameter, mean piston speed, and burnt gas properties, and S_L is the laminar flame speed [6, 7].

Substitution for the temperature dependent transport and thermodynamic properties in S_L and Re enables S_T to be written as [5]:

$$S_\mathrm{T} \quad C \left(\frac{NBSP}{T_\mathrm{b}^{1.67}}\right)^{0.4} (T_\mathrm{b}^{0.41} T_\mathrm{u}^{1.25}) \left(\frac{\mathrm{R}}{E} \quad \frac{X_\mathrm{f} F(\phi)}{\phi}\right)^{0.5} \exp \quad \frac{E}{2\mathrm{R}T_\mathrm{b}} \tag{23}$$

$$F(\phi) \quad \frac{1 \quad (1 \quad \beta)}{\phi} \text{ for } \phi \quad 1; \quad F(\phi) \quad 1 \quad \phi(1 \quad \beta) \text{ for } \phi \quad 1 \tag{24}$$

$$\beta \quad \frac{\mathrm{R}T_\mathrm{b}^2}{E(T_\mathrm{b} \quad T_\mathrm{u})} \tag{25}$$

Flame propagation

Frequently, the flame is assumed to propagate spherically from the one end of the cylinder (*i. e.*, spark plug). As the flame proceeds from one end to other the traveled portion of cylinder volume was assumed completely burnt, while the other as unburnt. If the flame speed is known from the equation, the distance traveled by flame was expressed by:

$$R_\mathrm{f} \quad \frac{S_\mathrm{T}\Delta\theta}{360N} \tag{26}$$

Knowing the radius of the flame front flame, burnt volume and surface areas are found out from the equations:

$$\text{Burnt area} = 2\pi R_\mathrm{f}^2 \tag{27}$$

$$\text{Burnt volume} = \frac{2}{3}\pi R_\mathrm{f}^3 \tag{28}$$

As all the quantities on the right hand side of eq. (22) are known the temperature can be found out and by the use of eq. (15) the corresponding pressure is estimated.

Mass fraction

The mass fraction is calculated using the following equation [2]:

$$\frac{\mathrm{d}m_{\mathrm{b}}}{d\theta} \quad \rho_{\mathrm{u}} A_{\mathrm{fl}} S_{\mathrm{T}} \tag{29}$$

This process of combustion is assumed to be completed if the radius of flame front is greater than the bore of the cylinder where the mass fraction burnt is more than or equal to 98.5%.

Expansion process

The analysis of this process is similar to that of compression process except the constituents in the cylinder. Here the cylinder contains only burnt gases such as H_2O and some traces of H_2, O_2, and CO_2. The expansion process ends when the exhaust valve opens.

Experimental procedure

Experimental procedure

A setup consisting of a single cylinder, air cooled, four-stroke, spark ignition engine of 2.5 kW rated power and 3000 rpm of rated speed is coupled to an eddy current dynamometer. Since the engine is meant for gasoline operation, some modifications are done in the cylinder head, intake manifold and spark plug for hydrogen operation [8, 9]. The schematic diagram of the set-up is shown in fig. 2. The cylinder head of the engine was modified to accommodate a piezoelectric pressure transducer for in-cylinder pressure measurement. The intake manifold was replaced with a modified manifold. The ignition timing was adjusted for hydrogen operation. For conventional SI engine, spark timing is 28º bTDC. The spark timing was retarded for hydrogen operation, since it may result in pre-ignition and knocking. The hot spark plug used for gasoline operation was replaced with a cold spark plug for hydrogen operation for avoiding preignition of charge. In the cold spark plug, the heat travels faster from the center electrode to the cooler cylinder head. The spark gap was also reduced from 0.5 mm to 0.38 mm to reduce the spark intensity.

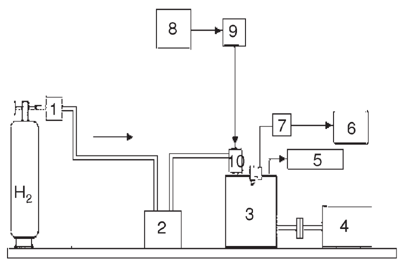

Figure 2. Schematic diagram of the experimental set-up
(1) Hydrogen flow meter, (2) Flame trap, (3) Engine, (4) Dynamometer, (5) Exhaust gas analyzer, (6) Cathode ray oscilloscope, (7) Charge amplifier, (8) Surge tank, (9) Air flow meter, (10) Intake manifold

Baseline readings were taken with gasoline as a fuel at a speed of 3000 rpm. A conventional carburetor was used for gasoline operation. An eddy current dynamometer was used to apply the load.

A regulator was used to bring down the pressure of hydrogen from 140 bar to 1.5 bar. A flow meter was connected to measure the flow rate of hydrogen which was placed in between the pressure regulator and flame trap. Charge amplifier was used to read the cylinder pressure data from a piezoelectric transducer. Cathode ray oscilloscope was used to indicate pressure *vs.* crank angle diagram.

Air was drawn from the surge tank through air flow meter. Air flow meter was used to measure the quantity of air. Both, hydrogen and air were supplied into the intake manifold. By varying the flow rate of hydrogen, the brake output was varied. Flame trap was placed in between hydrogen flow meter and intake manifold to avoid backfire problems. The minimum spark advance for best torque (MBT) was maintained at all the operating conditions. At each output, the combustion, performance, and emission characteristics were measured. HC, CO, and NO_x emissions were measured using a 5 gas analyzer.

Results & discussion

Cylinder pressure and temperature

From the motored case results, the maximum average cylinder temperature and pressure is attained at TDC position and the corresponding values are 542.73 K and 8.65 bar. The peak pressure and temperature values are obtained near the walls. This is because of the fact that, the air is confined to smaller area near the cylinder walls, resulting in a highly compressed state. The motored test was carried out under adiabatic wall boundary condition.

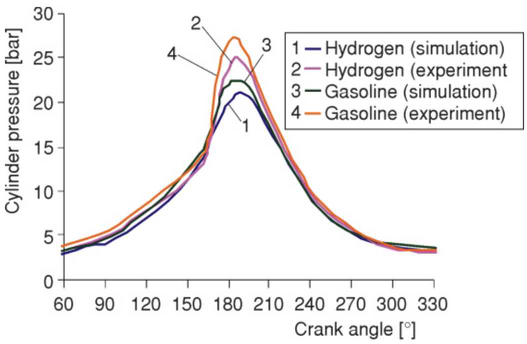

Figure 3. Pressure *vs.* crank angle diagram

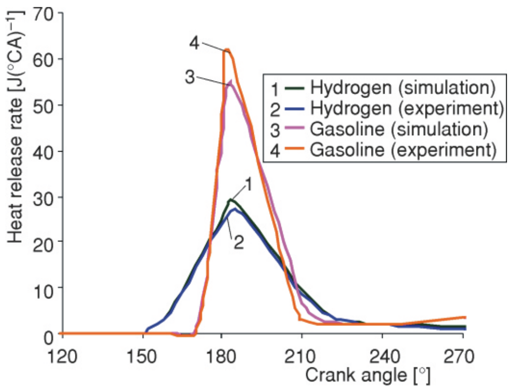

Figure 4. Variation of heat release rate with crank angle

Combustion parameters

Figure 3 shows the P-θ diagram for hydrogen and gasoline at the brake power output of 1.62 kW for their respective equivalence ratio. The simulated peak pressure values are compared with the experimental values. The rapid combustion in the hydrogen operation has sharp rises in the cylinder pressure and peak pressure values. From the experiment, the peak pressure value for hydrogen is 19% higher than that of gasoline. From the simulation, the peak pressure value for hydrogen is 21% higher than that of gasoline. The peak pressure value is higher due to faster burning rate. Figure 4 shows the variation of heat release rate for hydrogen and gasoline at the brake power output of 1.62 kW. The maximum heat release rate with hydrogen is around 54.8 J/°CA, where as in gasoline operation it is around 26.9 J/°CA, which is nearly double that of gasoline operation. This was found to be the major reason for the abrupt pressure rise [2]. The rate of heat release is higher because of higher burning rate of hydrogen. Also, it is noticed that combustion duration for hydrogen is lesser than gasoline.

Performance parameters

In the case of gasoline operation, the throttle was operated to vary the brake power output, while in the case of hydrogen the throttle was always set at the wide open condition and the equivalence ratio was changed. The maximum brake power output attained with gasoline was around 2.5 kW, whereas with hydrogen operation, it was around 1.62 kW. Hydrogen operation produced about 35% lesser power than gasoline. The equivalence ratio of 0.8 results in maximum brake power with hydrogen. Further attempts to increase the brake power output by increasing the equivalence ratio resulted in knocking. This is mainly due to an abrupt drop in the ignition energy of the hydrogen-air mixture to a very low value at these equivalence ratios. So, any hot spot in the engine can easily ignite the charge in the inlet manifold when the charge is close to stoichiometric.

Figure 5 shows the variation of equivalence ratio with brake power for hydrogen and gasoline operation. The minimum equivalence ratio was 0.4 at which stable engine operation was achieved, without misfire. Thus very lean operation is possible. A gasoline engine can not run with such a lean mixture. Normally, with lean mixtures, the combustion of gasoline will be too erratic and therefore engine will be operated at a considerably richer condition at all the operating points. With hydrogen, the highest equivalence ratio that could be used was about 0.8 which was limited by backfiring. Wide range of power outputs could be obtained with hydrogen merely by changing the equivalence ratio.

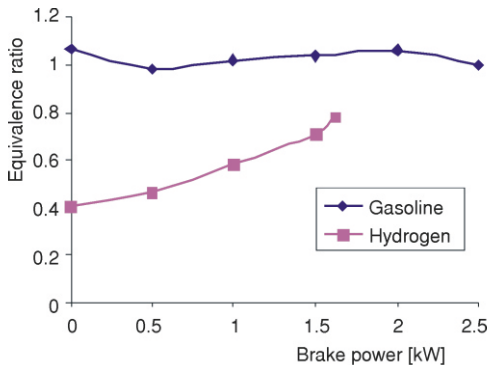

Figure 5. Variation of equivalence ratio with brake power

Figure 6 shows the variation of brake thermal efficiency with brake power output. It is observed that hydrogen operation is more efficient than that of gasoline at all operating points. With hydrogen, the maximum brake thermal efficiency was around 22% at the maximum power output, whereas for gasoline operation, it was around 16%. Even at low brake power outputs, the brake thermal efficiency is high with hydrogen operation. This is mainly because the engine was operated without a throttle and thus very low pumping losses were encountered. At higher brake power outputs, the flame speed increases as the equivalence ratio increases and thus nearly constant volume combustion is achieved with hydrogen, which results in higher brake thermal efficiency. Also, at all the operating conditions, the mixture is much leaner than that of gasoline resulting in improved brake thermal efficiency.

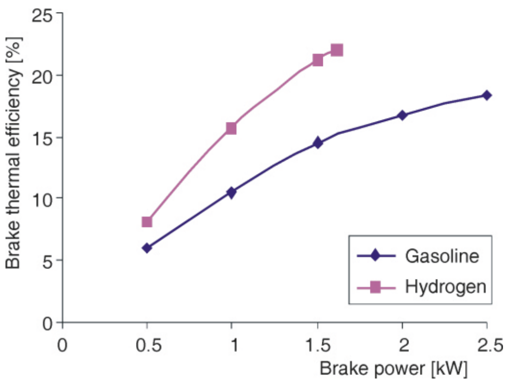

Figure 6. Variation of brake thermal efficiency with brake power

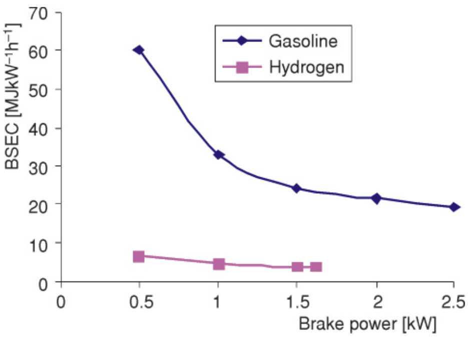

Figure 7. Variation of brake specific energy consumption with brake power

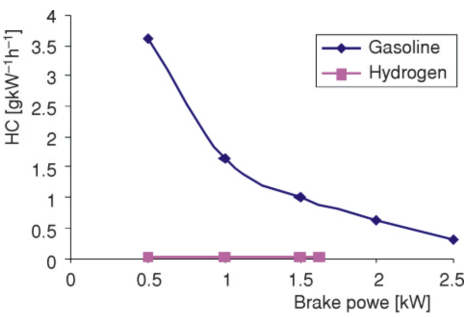

Figure 8. Variation of UBHC emissions with brake power

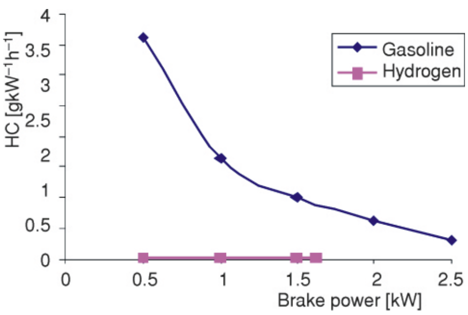

Figure 9. Variation of NO_x emission with brake power

The variation of brake specific energy consumption (BSEC) with brake power is shown in fig. 7. It is observed that, the brake specific energy consumption for hydrogen operation is lower over the entire region when compared to gasoline fueled operation. This is due to the higher calorific value of hydrogen based on mass basis. Also, the wide ignition limits of hydrogen make it possible to run the hydrogen fueled engine at very lean mixtures.

Emission parameters

No emission of CO or CO_2 was noticed during experiments with hydrogen. Only oxides of nitrogen and some traces of HC were found in the exhaust gas.

Figure 8 shows the variation of unburnt hydrocarbon emissions (UBHC) with brake power. The hydrogen fueled engine produces almost zero UBHC emissions, as the fuel does not contain any carbon particles. However, some traces of UBHC emissions were found because of the burning of the lubricating oil. A considerable amount of hydrogen enters into the crankcase due to blowby and reacts with the lubricating oil.

Figure 9 shows the variation of NO_x emission with brake power for hydrogen and gasoline operation [10, 11]. In the case of hydrogen, NO_x emissions are less upto a brake power output of 1.5 kW ($\phi = 0.7$). When the equivalence ratio increases beyond this value, the NO_x emission is found to increase significantly. At higher brake power outputs, equivalence ratio increases as flame speed increases and therefore higher peak pressures and temperatures are produced and results in higher NO_x emissions. At low brake outputs, the engine was operated at leaner mixtures. So, peak temperature is low compared with gasoline. Hence, NO_x emissions are less by 12%.

Conclusions

Based on the simulation and experimental study, the following conclusions are drawn.

From simulation, the maximum heat release rate for hydrogen is 60.2 J/°CA whereas for gasoline, it is 29 J/°CA. From the experimental investigation, the maximum heat release rate

for hydrogen and gasoline are 54.8 J/°CA and 26.9 J/°CA at the same brake output (1.62 kW). This higher heat release rate for hydrogen is due to higher burning rate.
At the same brake output, the peak pressure value for hydrogen is 27.32 bar which is 19% higher than gasoline (22.4 bar) obtained from simulation. From experimental investigation, the peak pressure value for hydrogen and gasoline are 25 bar and 21 bar. Due to higher burning rate, the higher peak pressure value is obtained for hydrogen. The difference between the simulation results and the experimental results are found to be only 2.24 bar.
When hydrogen was inducted along with air, the minimum equivalence ratio at which the engine operation was stable was 0.4. Beyond an equivalence ratio of 0.8, the engine could not be operated due to knocking.
The maximum brake power output attained with gasoline was around 2.5 kW, whereas with hydrogen operation, it was around 1.62 kW. So the hydrogen test engine produced about 35% lesser power than gasoline.

- At the maximum brake power output (1.62 kW) of hydrogen, the brake thermal efficiency of hydrogen and gasoline are 22% and 16%, respectively.
- The hydrogen fueled engine produces almost zero UBHC emissions, as the fuel does not contain any carbon particles. However, some traces of UBHC were found because of burning of the lubricating oil.

The NO_x emission is lesser compared with gasoline till an equivalence ratio of 0.7 and significantly increases beyond that point.

Nomenclature

A – area of the gases, [m^2]
A_{fl} – area of the flame front, [m^2]
B – bore diameter, [m]
C – mean piston speed, [ms^{-1}]
E – activation energy of hydrogen [kcalkmol^{-1})
h – heat transfer coeeficient, [–]
h_u – heat transfer coefficient of unburned mixture, [–]
h_b – heat transfer coefficient of burned mixture, [–]
m_b – mass of the burnt mixture, [kg]
m_u – mass of the unburnt mixture, [kg]
N – speed of the engine, [rpm]
P – gas presure inside the cylinder, [bar]
Pm – motor pressure, [Nm^{-2}]
Pr – pressure at the reference state, [Nm^{-2}]
Q – heat of the gases
R – universal gas constant, [Jkg^{-1}K^{-1}]
Re – Reynold's number, [$U_{in}\nu/\lambda_f$], [–]
R_f – radius of flame front, [m]
r – compression ratio, [–]
S – stroke length, [–]
S_L – laminar flame speed, [ms^{-1}]
S_T – turbulent flame speed, [ms^{-1}]
T_b – temperature of the burned gases, [K]
T_u – temperature of the unburned gases, [K]
V – volume of the gases, [m^3]
V_{disp} – displacement volume, [m^3]
V_h – stroke volume, [m^3]
V_r – volume at the reference state, [m^3]
X_f – mole fraction of fuel, [–]
y_i – mole fraction of the species, [–]

Greek letters

β – variable, [–]
θ – crank angle, [°]
ϕ – equivalence ratio, [–]
γ – ratio of the specific heat, [–]
ρu – density of the unburnt mixture [kgm^{-3}]

Subscripts

b – burnt
u – unburnt

References

[1] Ghazi, A. Karim, Hydrogen as a Spark Ignition Engine Fuel, *International Journal of Hydrogen Energy, 28* (2003), 7, pp. 569-577

[2] Shudoa, T., Suzukib, H., Applicability of Heat Transfer Equations to Hydrogen Combustion, *JSAE Review, 23* (2002), pp. 303-308
[3] Jehad, A. A, Yamina, *et al*., Effect of Combustion Duration on the Performance and Emission Characteristics of a Spark Ignition Engine Using Hydrogen as a Fuel, *International Journal of Hydrogen Energy, 25* (2000), 6, pp. 581-589
[4] Ma, J., *et al*., Simulation and Prediction on the Performance of a Vehicle's Hydrogen Engine, *International Journal of Hydrogen Energy, 28* (2003), 1, pp. 77-83
[5] Maher, A. R., Al-Baghdadi, S., A Prediction Study of the Effect of Hydrogen Blending on the Performance and Pollutants Emission of a Four Stroke Spark Ignition Engine, *International Journal of Hydrogen Energy, 24* (1999), 4, pp. 363-375
[6] Tirkey, J. V., *et al*., Integrated Gas Dynamic and Thermodynamic Computational Modeling of Multicylinder 4-Stroke Spark Ignition Engine Using Gasoline as a Fuel, *Thermal Science, 13* (2009), 3, pp. 113-130
[7] Maher, A. R., *et al*., A Prediction Study of a Spark Ignition Supercharged Hydrogen Engine, *Energy Conversion and Management, 44* (2003), 20, pp. 3143-3150
[8] Nagalingam, B., Dubel, M., Schmillen, K., Performance of the Super Charged Spark Ignition Hydrogen Engines, SAE paper 831688, 1983
[9] Prabhu Kumar, G. P., *et al*., Theoretical and Experimental Studies in a Spark Ignited Hydrogen Fueled Spark Ignition Engines, *Proceedings*, 8^{th} National Conference on I. C. Engines and Combustion, Trivandrum, Kerala, India, 1983
[10] Khajuria, P. R., Mathur, H. B., An Analytical and Experimental Study of NO_x Emissions of Hydrogen Fueled S. I. Engine, *Proceedings*, 8^{th} National Conference on I. C. Engines and Combustion, Trivandrum, Kerala, India,1983
[11] Mobasheri, R., Fotrosy, Y., Jalaifar, S., Modeling of Spark Ignition Engine Combustion: A Computational and Experimental Study of Combustion Process Effects on NO_x Emissions, *Asian Journal of Applied Sciences, 2* (2009), 4, pp. 318-330

Paper submitted: June 11, 2009
Paper revised: October 27, 2009
Paper accepted: June 5, 2010